LETTER • OPEN ACCESS

Establishing sustainable sediment budgets is critical for climate-resilient mega-deltas

View the article online for updates and enhancements.

ENVIRONMENTAL RESEARCH
LETTERS

LETTER

Establishing sustainable sediment budgets is critical for climate-resilient mega-deltas

G Vasilopoulos[1,*] ![ORCID], Q L Quan[1,2], D R Parsons[1], S E Darby[3], V P D Tri[4], N N Hung[2], I D Haigh[5] ![ORCID], H E Voepel[3], A P Nicholas[6] and R Aalto[6]

1   Energy and Environment Institute, University of Hull, Hull, United Kingdom
2   Southern Institute of Water Resources Research, Ho Chi Minh City, Vietnam
3   School of Geography and Environmental Science, University of Southampton, Southampton, United Kingdom
4   College of Environment and Natural Resources, Can Tho University, Can Tho, Vietnam
5   Ocean and Earth Science, University of Southampton, National Oceanography Centre Southampton, Southampton, United Kingdom
6   College of Life and Environmental Sciences, University of Exeter, Exeter, United Kingdom
*   Author to whom any correspondence should be addressed.

E-mail: g.vasilopoulos@ac.uk

Abstract

Many of the world's major river deltas face a sustainability crisis, as they come under threat of increases in salinity and the extent of tidal zones forced by combinations of sea-level rise, changes in river discharge and channel geometry. The relative contribution of these factors to future increases in tidal extent remains unconstrained, with most prior work emphasising the role of climate-driven sea-level rise. Here we use new field data from the Mekong delta to measure variations of river discharge and changes of channel geometry, and project them into the future. We combine these with projections of future sea-level rise into a 2D hydrodynamic numerical model and quantify the influence of the different driving factors on future tidal extension into the delta. We show that within the next two decades, tidal extension into the Mekong delta will increase by up to 56 km due to channel deepening (92%), dominantly driven by anthropogenic sediment starvation. Furthermore, even under strong mitigation scenarios, sediment starvation still drives a long-term commitment to future tidal extension. Specifically, by 2098 eustatically rising sea-levels are predicted to contribute only modestly to the projected extension. These findings demonstrate the urgent need for policy makers to adopt evidence-based measures to reverse negative sediment budgets that drive tidal extension into sediment starved deltas.

1. Introduction

The world's deltas occupy less than 1% of the global land surface, but 4.5% of the global population lives on them (Edmonds *et al* 2020). The ecosystem services that deltas support provide a range of socio-economic functions (Szabo *et al* 2016) that underpin global food security (Smajgl *et al* 2015). However, many large deltas are being drowned (Syvitski *et al* 2009) due to rapid relative sea-level rise, which in 46 of the world's largest deltas averages rates of more than 6 mm yr^{-1} (Tessler *et al* 2018), presenting a major threat to these systems (Anthony *et al* 2015). Rapidly rising relative sea-levels are driven by a range of compound pressures including

eustatic sea-level rise, accelerating subsidence and sediment starvation (Ericson *et al* 2006, Syvitski 2008, Vörösmarty *et al* 2009). Some studies estimate that by 2100 greenhouse gas-driven eustatic sea-level rise alone will increase the areas at risk of flooding in the world's deltas by more than 50% (Syvitski *et al* 2009), exacerbating saline intrusion into their sensitive ecosystems (Smajgl *et al* 2015, Ensign and Noe 2018). Meanwhile, delta subsidence, driven by compaction of sedimentary strata (Törnqvist *et al* 2008) is also being accelerated due to increased rates of ground water extraction (Zhang *et al* 2008b, Erban *et al* 2014) in many locations. Furthermore, many large deltas are also sediment starved (Dunn *et al* 2019) resulting from declines in the supply of fluvial sediment

caused by upstream dam construction (Dai and Liu 2013, Kondolf *et al* 2014), rapid and accelerating sand mining (Bravard *et al* 2014, Hackney *et al* 2020), and the construction of flood embankments (Vörösmarty *et al* 2009, Auerbach *et al* 2015, Chapman *et al* 2017, Tamura *et al* 2020). Such sediment starvation potentially compromises the ability of deltas to offset rising sea levels through sediment deposition (Syvitski *et al* 2009, Giosan *et al* 2014). The combined influence of these multiple pressures of relative sea-level rise and changes in water and sediment discharges, driven by global warming (Lan *et al* 2016) and catchment engineering (Vörösmarty and Sahagian 2000), directly impacts the sensitive balance between fluvial and tidal forces that governs tidal extent (TE) in large deltas. TE is defined here as the region of the delta where flow discharge is dominated by tidal forcing. This is important because TE regulates saline intrusion (Eslami *et al* 2019), water and sediment routing (Nienhuis *et al* 2018), and channel stability (Zhang *et al* 2017). Disentangling the relative impacts of the distinct pressures influencing TE, and especially their future evolution, is pertinent to generating evidence-based policy that could underpin adaptation and mitigation strategies for exposed deltas.

We focus on the Mekong delta because it is classified by the Intergovernmental Panel on Climate Change (IPCC) as one of the three most vulnerable deltas globally (Parry *et al* 2007) and because it is representative of other large deltas not only in terms of the multiple drivers of change it is experiencing, but also in its response to these pressures. For example, similar to many other deltas (Dunn *et al* 2019), the supply of fluvial sediment to the Mekong has experienced a major decline, from 160 Mt yr^{-1} in the 1980's (Milliman and Meade 1983) to 87 Mt yr^{-1} in 2005 (Darby *et al* 2016). These declining rates of fluvial sediment supply have been attributed to the effects of shifting tropical cyclone tracks (Darby *et al* 2016) as well as extensive river impoundment and hydropower development across the Mekong's catchment (Kondolf *et al* 2014). Furthermore, many sections of the river and its delta have been subject to intensive sand mining activities, with previous studies documenting annual removal rates in excess of 50 Mt yr^{-1} (Bravard *et al* 2013) and a recent study suggesting that unregulated sand mining is also occurring (Jordan *et al* 2019). This produces a significant net negative sediment budget when compared to sand influx rates of 6.2 ± 2.0 Mt yr^{-1} at the delta apex (Hackney *et al* 2020). As a result, similar to other large deltas such as the Chao Phraya (Winterwerp *et al* 2005, Saito *et al* 2007), Pearl (Zhang *et al* 2008a), Yangtze (Yang *et al* 2015) and Yellow (Wang *et al* 2010), the Mekong is subject to severe, anthropogenically-driven, sediment starvation, resulting in rapid and extensive channel bed level lowering (Brunier *et al* 2014), which in the recent past has led to an intensification of salt-water intrusion (Eslami *et al* 2019), and reversing

prograuation of the channel mouths (Tamura *et al* 2020). Synchronous to this anthropogenically-driven channel bed level lowering, the delta is also experiencing: (a) a eustatic rising of sea-levels, forced by global warming, which for the Mekong delta region is projected to be up to 1 m by 2100 (RCP 8.5) (relative to 1998) (see supplementary figure 8 (available online at stacks.iop.org/ERL/16/064089/mmedia)), and (b) an anthropogenically accelerated sediment compaction which is projected to give cumulative subsidence of up to 1.4 m by 2100 (relative to 1990) (Minderhoud *et al* 2020). Here we use new field data and aligned numerical hydrodynamic modelling to develop the first analysis of the combined influence of future (to 2098) eustatic sea-level rise, river discharge and delta channel changes, the latter partitioned into sediment loss and land subsidence, on tidal extension in the Mekong delta.

2. Data and methods

We quantify historical bed-level lowering of the principal distributary channels of the Vietnamese Mekong Delta (VMD) by comparing successive bathymetric surveys for the years 1998, 2008 and 2018. We then propagate the identified trends of bed-level changes 20 years forward by assuming a 'business as usual' evolution of pressures and generate potential future alternate delta analogues. We develop a two-dimensional hydrodynamic numerical model (based on the varying delta topographies) and undertake a series of numerical experiments ($n = 105$) to explore the response of delta hydraulics under a range of compound pressures, accounting for co-variations in: (a) eustatic sea-level rise; (b) river discharge, and; (c) channel bed lowering. We analyse annual time series of predicted hourly water discharges at 100 locations across the delta channel network to quantify tidal extension for each one of the scenarios investigated.

2.1. Historical bathymetric surveys
Historical bathymetric surveys (Brunier *et al* 2014) were obtained from the Mekong River Commission (www.mrcmekong.org). These surveys consist of point data for the years 1998 and 2008 and cover approximately 51% (432 km^2) of the delta's principal channels. They include depth measurements with a depth uncertainty of ± 0.2 m for every 10 m which generates a mean vertical error of 0.19 and 0.21 m for the 1998 and 2008 datasets, respectively. They are referenced to the World Geodetic System 1984 (WGS84) and the Ha Tien 1960 mean sea level (MSL) datum. We adopted the Universal Transverse Mercator (UTM) coordinate system and projected the geographic coordinates into WGS84 UTM 48 N. We verified historic MRC data and procedures used for vertical referencing, and then converted the elevation values from Ha Tien 1960 to the Hon Dau 1992 MSL

by subtracting the 0.167 m offset from each reported elevation. Hon Dau is the vertical datum currently used in Vietnam.

2.2. Contemporary bathymetric survey

Our contemporary bathymetry was obtained from a delta-wide survey conducted in May 2018. We used two vessels, equipped with identical single beam echo-sounding (SBES) systems consisting of a Garmin GT20-TM sonar transducer, fully submerged ($\sim$0.5 m) below the water surface, linked to a global positioning system (GPS). Depending on channel depth, we altered the sonar pulse frequency between 800 and 455 kHz with beam angles of 1.6° and 2.5°, respectively. Data were recorded at a frequency of 1 Hz; vessel speed was kept below 20 km h^{-1} to minimise air entrainment and data noise. Garmin does not specify a measurement error for their system, hence we adopt the same vertical uncertainty as for the historical data, which generates a mean vertical error of 0.25 m for the 2018 dataset. We henceforth propagate the mean errors of the historical and 2018 surveys into our volumetric differencing and subsequent channel bed level lowering rates. A limited part of the principal delta channels (145 km^2 out of 854 km^2) had already been thoroughly surveyed in 2014 (supplementary figure 1). We surveyed these areas following a straight course along the channels to identify general trends of change within the 4 year period (see later). We then concentrated our efforts to extensively survey the remaining areas (709 km^2 out of 854 km^2), that had not been surveyed since 2008. To optimise channel coverage, our survey tracks followed oblique cross-sections crossing from bank to bank, thereby forming open triangles with their apexes spaced approximately two channel widths apart.

Acoustic recordings were converted into projected (WGS84 UTM 48N) coordinates and measurements of total water depth. The latter were transformed to elevations using hourly water level recordings from the Vietnamese hydrological agency's network of water level monitoring stations (supplementary figure 1), referenced to the Hon Dau MSL. We compared the bed elevations measured in 2014 with the corresponding ones measured in 2018 and found that within the 4 year period the landward section of the principal Mekong had been lowered by 2.9 m on average, whereas a limited section of the Bassac had been raised by 0.6 m on average. We adjusted the 2014 data accordingly and used them to augment our 2018 survey data.

2.3. Principal channel bed surfaces

We interpolated channel bed surfaces from the survey data and compared historical and contemporary channel morphology. To account for the anisotropy of channel bed elevations, due to flow directionality (Merwade *et al* 2006, Legleiter and Kyriakidis 2008),

a flow-oriented anisotropic kriging interpolation was employed. We chose a 50 m cell size for the resulting contemporary and historical maps of channel bed elevations (figure 1 and supplementary figure 2).

Surface differencing of contemporary and historical maps (see section 3 and supplementary figure 2) highlighted spatial trends for channel bed-level lowering, with change being most prominent in the landward sections, whereas in areas very close to the shore almost no change was observed (figure 1(a)). These patterns were summarised by extracting linear trends of laterally averaged channel change for the principal Mekong (section indicated as MM' in supplementary figure 2(c)) and Bassac (section indicated as BB' in supplementary figure 2(c)) (supplementary figure 3) channels. Trends of channel bed-level lowering were interpolated spatially into raster maps representing the historical trend of bed-level changes across the principal channel network (supplementary figures 4(a) and (b)).

2.4. Hydrodynamic model

A 2D hydrodynamic model (supplementary figure 5) was developed using the Danish Hydraulics Institute's MIKE21 FM modelling suite, using a combination of regular and flexible mesh elements ($n = 244\,000$). Simulations were undertaken using a high-performance computing system, with a full year simulation requiring approximately 1.5 d to complete. Our modelling simulations included a hydrodynamic component, with channel bathymetry remaining constant during scenario runs but varied between scenarios as described in section 2.5.

The domain topography (supplementary figure 5) was based on the 2018 measured channel bed elevations, augmented with nearshore bathymetric data provided by the Southern Institute of Water Resources Research in Vietnam, surveyed in 2009 using a Teledyne ODOM Hydrotrac echosounder coupled with a Trimble SPS351 GPS, and offshore bathymetric data obtained in 2012 from navigational charts. Our 2018 bathymetric survey overlaps with a limited part of the nearshore bathymetries obtained in 2009. Comparison of the two datasets showed a mean deepening of these areas by 0.095 m between 2009 and 2018 which, in the context of the overall deepening in excess of 1.6 m for the 2008–2018 period, we consider negligible. Our 2018 surveys did not extend offshore to assess the quality of the navigational chart bathymetries. The landward boundary conditions were forced by hourly time series of river discharge as measured at the Tan Chau and Chau Doc gauging stations (supplementary figure 5) that covered a full year. The sea boundary was forced by tidal levels at hourly intervals that also cover a full year. Tidal levels were estimated from the global ocean tide model DTU10 (Cheng and Andersen 2010) but calibrated against observations at three proximal

monitoring stations (Gan Hao, Ben Trai and Vung Tau) (supplementary figure 5) operated by the Southern Region Hydrometeorological Centre in Vietnam.

To ensure the robust calibration and validation of our model, we used two distinct sets of boundary conditions corresponding to the years 2016 (for model calibration) and 2018 (for model validation). 2018 represents a high flood year with above-average mean annual discharge values equal to 11 767 m^3 s^{-1} (2001–2018 mean annual flow = 10 140 m^3 s^{-1}) and 2553 m^3 s^{-1} (2001–2018 mean annual flow = 2439 m^3 s^{-1}) for Tan Chau and Chau Doc, respectively. The year 2016 is close in time to our 2018 survey, but represents a dry year with below-average mean annual discharge values, equal to 8963 m^3 s^{-1} and 1940 m^3 s^{-1} for Tan Chau and Chau Doc, respectively. Calibration was performed by adjusting the model's hydraulic roughness, running a full year simulation (with boundary conditions for 2016) and comparing model predictions of hourly water levels against observations from monitoring stations distributed across the delta (see supplementary figure 5 for locations). We calculated the Nash–Sutcliffe model efficiency coefficient (Nash and Sutcliffe 1970) (NSE) to assess model performance (supplementary figure 6). We then validated our model by conducting a full year simulation run using the 2018 channel survey with 2018 boundary conditions, again computing NSE values to assess model performance (supplementary figure 7).

2.5. Scenarios

We designed a series of 105 simulation scenarios to explore the response of delta hydraulics under a range of compound pressures.

For eustatic sea-level rise (a), we used seven scenarios, based on projections from the Warming Acidification and Sea level Projector (WASP) (Goodwin *et al* 2017, Oppenheimer *et al* 2019) for the grid point closest to the Mekong delta, which are broadly consistent with the IPCC Fifth Assessment Report (AR5) projected range (Church *et al* 2013). We chose to assess 0.06, 0.1, 0.2 and 0.25 m of sea level rise (relative to 1998) by the years 2008, 2018, 2031 and 2038, respectively. These levels of sea-level rise correspond approximately to average projections across all RCPs for this period (supplementary figure 8). We also explored the effect of a 0.5 m sea-level rise which is predicted by all RCPs (but for different years) and that of a 1 m SLR, that reflects the upper end of the RCP 8.5 by 2100. Within the hydrodynamic model, we vertically offset the sea boundary (which is based on the 1998 tidal time series) by the specific mean sea-level rise scenarios.

The effects of river discharge variability (b) were assessed using three distinct river flow discharge data sets. Specifically, we used hourly observations of river discharge at Tan Chau and Chau Doc that covered the entire years 2013, 2010 and 2001 (supplementary

figure 8). We selected these years because their mean annual discharge values are close to the median, lower and upper bounds, respectively, of the range of discharges observed during 2001–2018.

Finally, to explore the effects of channel bed-level lowering (c) we repeated all simulations with five different bathymetries corresponding to historical, contemporary and three future projected conditions. The three future scenarios were developed to represent the potential evolution of channel geometry under different mitigation approaches. The first mitigation scenario (scenario M1) is a hypothetical scenario in which effective regulation is implemented immediately to maintain the delta channel geometry at its contemporary (i.e. 2018) state and as such matches the contemporary channel bed levels (figure 1(a)). Scenario M2 corresponds to a hypothetical trajectory where mitigation is deferred and the delta channels continue to lower their beds (at their present rates) until 2028, when further bed-level lowering is halted. We produced M2 (figure 1(c)) by subtracting the 2008–2018 map of channel bed-level change (supplementary figure 4(b)) from the contemporary (2018) channel survey (figure 1(a)). The channel bed levels of M2 are on average 1.4 m lower relative to 2018. Scenario M3 represents a hypothetical trajectory in which mitigation is delayed until 2038. We produced M3 (figure 1(c)) by subtracting the 2008–2018 raster map of bed-level change (supplementary figure 4(b)) from M2. The channel bed levels of M3 are on average 2.8 m lower relative 2018. We chose not to extrapolate scenarios of channel bed-level lowering beyond 2038 because of uncertainties surrounding both the extent of sediment reserves within the VMD and the future demand for sand. Due to missing areas in the historical datasets (supplementary figures 2(a) and (b), we used the 2018 channel survey and historical trajectories to develop historical analogues of the entire delta for 1998 and 2008. The 2008 historical delta analogue (HA2) (supplementary figure 4(d)), with channel bed levels on average 1.4 m higher than the 2018 bathymetry, is derived by adding the 2008–2018 raster map of channel bed level change to the contemporary (2018) channel survey. The 1998 historical delta analogue (HA1) (supplementary figure 4(c)), with channel bed levels on average 2.6 m higher than the contemporary bathymetry, is derived by adding the 1998–2008 raster map of channel bed level change to HA2.

3. Results

3.1. Anthropogenic channel bed-level lowering

Comparison of the interpolated channel bed surfaces for 1998, 2008 and 2018 reveals a substantial, accelerating, bed-level lowering of the delta channels. Specifically, our data show a mean bed-level lowering of 2.5 m (σ = 3.9 m) since 1998, with change being most prominent in the landward sections, whereas
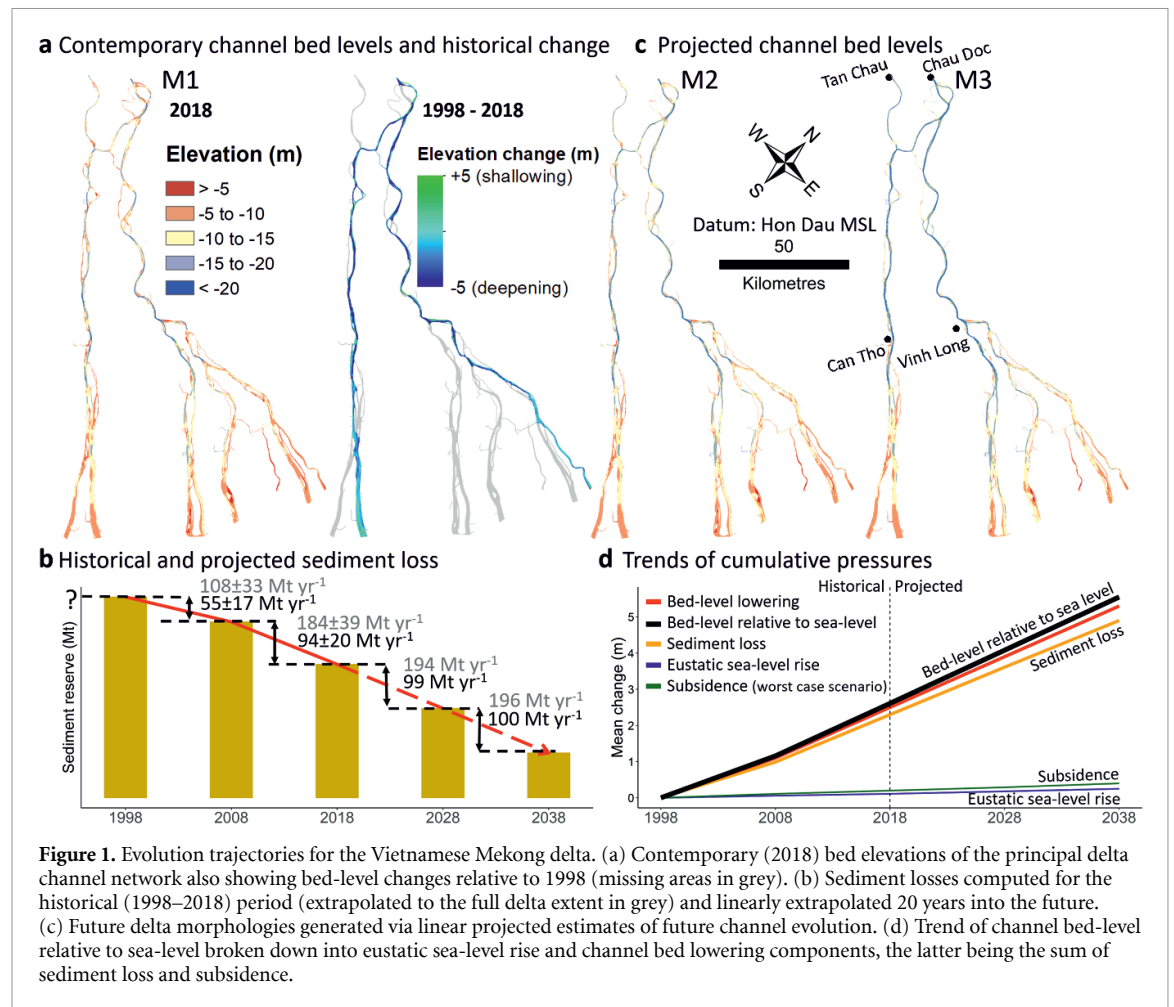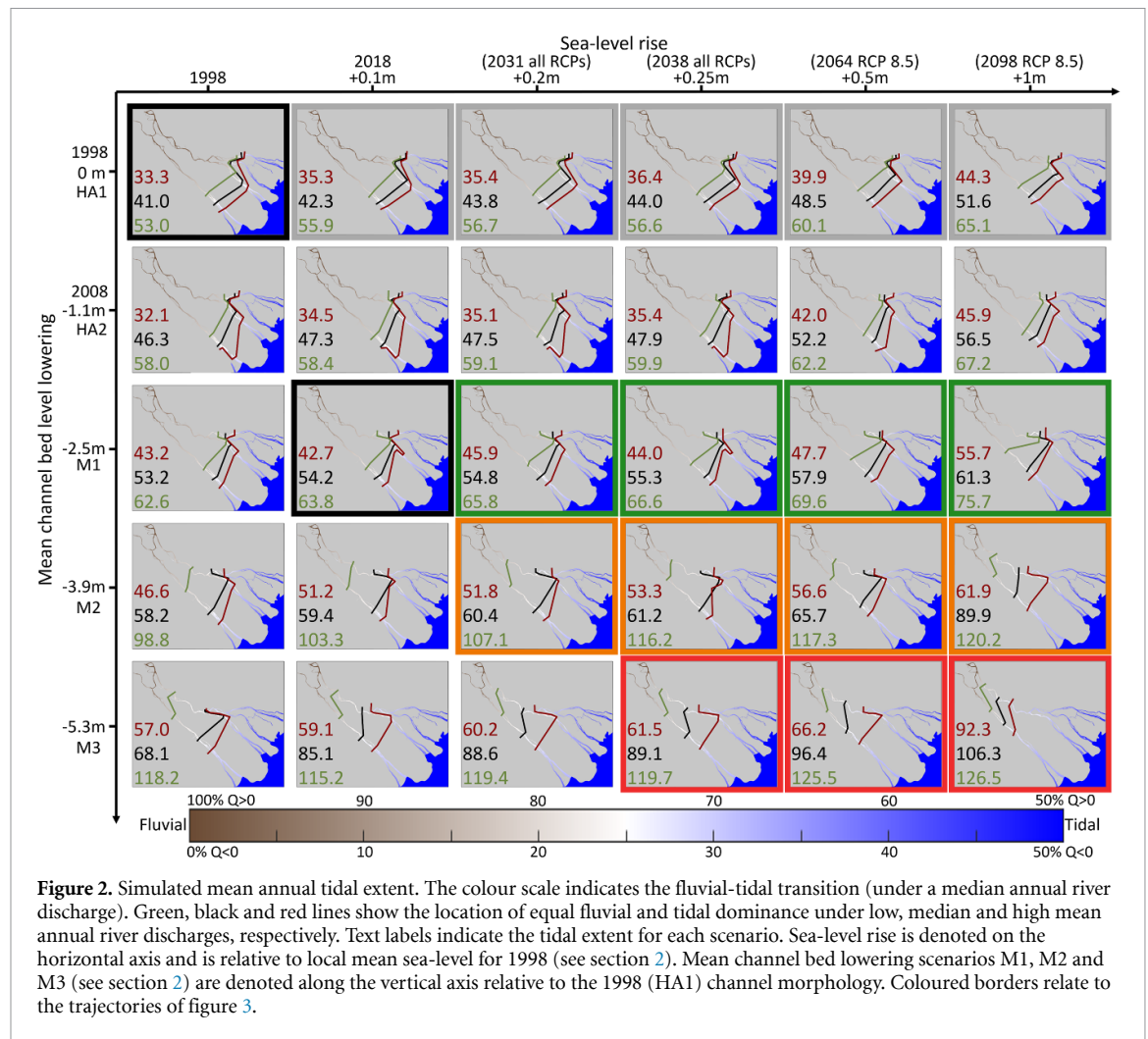
Figure 1. Evolution trajectories for the Vietnamese Mekong delta. (a) Contemporary (2018) bed elevations of the principal delta channel network also showing bed-level changes relative to 1998 (missing areas in grey). (b) Sediment losses computed for the historical (1998–2018) period (extrapolated to the full delta extent in grey) and linearly extrapolated 20 years into the future. (c) Future delta morphologies generated via linear projected estimates of future channel evolution. (d) Trend of channel bed-level relative to sea-level broken down into eustatic sea-level rise and channel bed lowering components, the latter being the sum of sediment loss and subsidence.

in areas very close to the shore almost no change was observed (figure 1(a)). This is likely due to an increasing sediment influx from the coast (Ha *et al* 2018) and the increased sand mining activity that is particularly concentrated in the landward reaches of the delta. Comparisons at decadal intervals reveal that the bed levels of the common areas (51% of the principal delta channels) were lowered by 0.9 m (σ = 3.2 m) during 1998–2008, and by 1.6 m (σ = 2.9 m) during 2008–2018 (supplementary figure 2). Minderhoud *et al* (2020) have quantified a mean cumulative subsidence for the Mekong delta plain of 0.2 m for the period 1990–2018. Therefore, at least 2.3 out of the 2.5 m (92%) of bed-level lowering that we quantify here cannot be explained by subsidence and must be as a result of sediment loss. Accounting for this modest subsidence generates volumetric sediment loss estimates of approximately $341 \times 10^6 \pm 97 \times 10^6$ m³ and $584 \times 10^6 \pm 112 \times 10^6$ m³ which, assuming a bulk density of 1600 kg m⁻³, corresponds to 546 ± 155 Mt and 934 ± 195 Mt for the 1998–2008 and 2008–2018 periods, respectively. Extrapolating the sediment losses found on the common areas across the entire principal channel network, suggests that these channels lost sediment at average rates of 108 ± 33 Mt yr⁻¹ during 1998–2008 and 184 ± 39 Mt yr⁻¹ during

2008–2018 (figure 1(b)). Combining the observed trajectory of bed-level lowering with the 2018 survey, taking into consideration the spatial variability of quantified changes (see section 2 and supplementary figures 3 and 4), we project the future morphology of the delta channels (figure 1(c)) by assuming a 'business as usual' evolution of compound pressures, giving an estimated bed-level lowering of 5.3 (3.9) m by 2038 (2028), relative to the 1998 analogue.
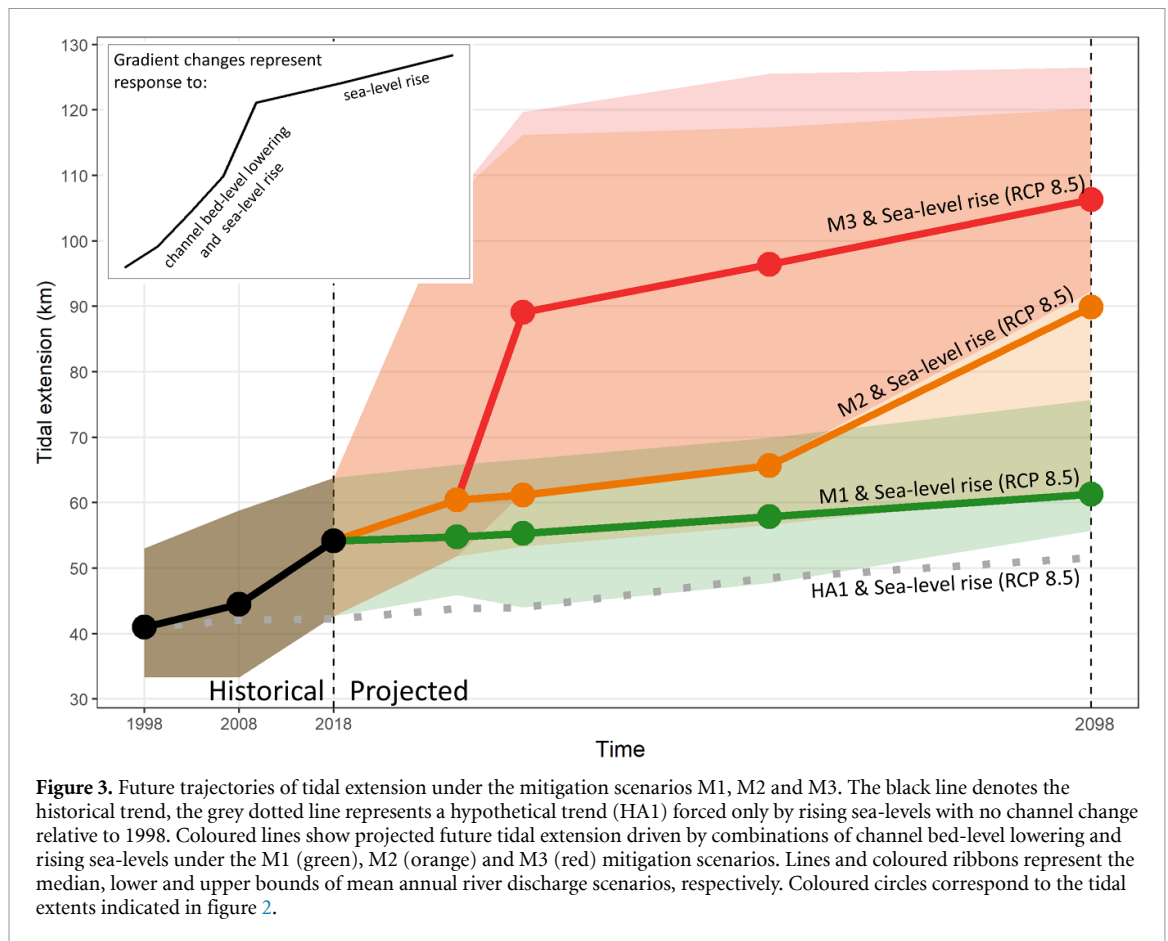
The average GHG-driven sea-level rise is projected as 0.25 m in 2038, relative to 1998 regional sea levels (figure 1(d) blue line), across all RCP scenarios we consider here (supplementary figure 8). In contrast, the linear projected channel geometry for 2038 is 5.3 m lower than in 1998 (figure 1(d), red line) suggesting that the channel beds in 2038 will be 5.55 m lower with respect to sea-level than they were in 1998 (figure 1(d), black line). The cumulative subsidence for 2038 is projected to be 0.4 m by 2038 (Minderhoud *et al* 2020). Therefore, the vast majority of bed-level lowering in our scenarios for the recent past (2.3 of 2.5 m between 1998 and 2018) and future (2.6 of 2.8 m between 2018 and 2038) is attributable to anthropogenically-driven sediment loss (figure 1(d), orange line) under the combined influence of reduced sediment supply from the catchment and excessive river-bed mining.

Figure 2. Simulated mean annual tidal extent. The colour scale indicates the fluvial-tidal transition (under a median annual river discharge). Green, black and red lines show the location of equal fluvial and tidal dominance under low, median and high mean annual river discharges, respectively. Text labels indicate the tidal extent for each scenario. Sea-level rise is denoted on the horizontal axis and is relative to local mean sea-level for 1998 (see section 2). Mean channel bed lowering scenarios M1, M2 and M3 (see section 2) are denoted along the vertical axis relative to the 1998 (HA1) channel morphology. Coloured borders relate to the trajectories of figure 3.

3.2. Anthropogenically-driven tidal extension

The hydrodynamic model was used to explore 105 scenarios (90 are shown in figure 2), spanning a wide range of compound pressures. Simulated water discharge values at 1 h intervals at 100 locations across the delta (supplementary figure 9) show strong seasonal variability, driven by the monsoon-governed variations in river discharge, and hourly fluctuations governed by the tidal forcing. We adopted the convention that, under complete tidal dominance the flow would vary equally between positive and negative (inversed flow) discharge values (50% $Q > 0$), resulting in a net zero discharge over a full year, whereas a 75% $Q > 0$ represents the zone where fluvial and tidal forces equalise. We calculate the ratio of positive and negative discharge at each one of the 100 study locations and used this ratio to map the transition between fluvial and tidal dominance across the delta. We quantify the TE for each scenario by measuring the mean distance between the location of equal tidal and fluvial dominance (75% $Q > 0$) and the channel mouths ($n = 7$). Henceforth we report values of TE corresponding to the median (2013) river discharge, values for the lower (2001; wet year) and upper (2010; dry year) bounds are provided in figure 2.

The simulated average TE into the delta in 1998 was 41 km. Our simulations show that if the channel geometry had been maintained at 1998 conditions (HA1), the TE would have increased by only 1.3 km landward (TE = 42.3 km) during 1998–2018 and an additional 9.3 km (TE = 51.6 km) during 2018–2098, driven solely by the eustatically rising sea-levels (figure 2, grey panels) predicted by the RCPs. However, for the simulations in which the bed-level lowering during 1998–2018 is included, the landward increase of TE was extended by an additional 13.2 km, so that its predicted location by 2018 was 54.2 km from the channel mouths. Should immediate (2018) action be taken to halt channel deepening (scenario M1), the TE is predicted to increase a further 7.1 km landward (TE = 61.3 km) by 2098 due to eustatic sea-level rise (figure 2, green panels). In the M1 scenario, the TE (TE = 61.3 km) predicted in 2098 reaches almost 10 km further landward than the HA1-based equivalent (TE = 51.6 km). However, if channel degradation continues for another decade (scenario M2), the predicted TE in 2098 is 89.9 km, 35.7 km further inland than in 2018 (figure 2, orange panels). Moreover, if channel degradation is not halted until 2038 (scenario M3) the TE is predicted to more than

Figure 3. Future trajectories of tidal extension under the mitigation scenarios M1, M2 and M3. The black line denotes the historical trend, the grey dotted line represents a hypothetical trend (HA1) forced only by rising sea-levels with no channel change relative to 1998. Coloured lines show projected future tidal extension driven by combinations of channel bed-level lowering and rising sea-levels under the M1 (green), M2 (orange) and M3 (red) mitigation scenarios. Lines and coloured ribbons represent the median, lower and upper bounds of mean annual river discharge scenarios, respectively. Coloured circles correspond to the tidal extents indicated in figure 2.

double by 2098 (TE = 106.3 km), an increase of 52 km relative to 2018 (figure 2, red panels).

These trajectories, showing the potential future tidal extension within the delta under different drivers of change, are summarised in figure 3. The VMD is subjected to two groups of pressures of different magnitude. GHG-driven sea-level rise forces a slow, progressive, tidal extension of ∼0.1 km yr^{-1} (figure 3, grey dotted line). However, channel bed-level lowering, dominated by sediment starvation during the last 20 years, forces a much more rapid (0.5 km yr^{-1}) tidal extension landward (figure 3, black line). If the process of bed-level lowering continues unmitigated, the TE in 2098 is projected to be double that in 2018. Our simulations also show abrupt accelerations of the landward increase of the TE, interpreted here as being related to delta topology. Since the delta is increasingly bifurcated downstream (Edmonds and Slingerland 2008), and because channel widths increase seaward where tides become more dominant (Nienhuis *et al* 2018), both the number of distributary channels and the total channel cross-sectional area decrease landward (supplementary figure 10). Thus, as the TE stretches further landward, fewer and narrower channels exist to attenuate tidal energy. This mechanism creates a positive feedback which expands the TE further landward. Considering our historical trajectory (figure 3, black line) in relation to the delta topology (supplementary figure 10) suggests

that channel narrowing further exacerbated the tidal extension between 2008 (TE = 44.5 km) and 2018 (TE = 54.2 km). Our future trajectories will also similarly accelerate should the TE become greater than 70 km, which falls within a transition zone (60–90 km) of acute reduction of total cross-sectional area and number of distributary channels (supplementary figure 10). This key distance of 70 km is also close to the major cities of Can Tho (c. 75 km) and Vinh Long (c. 80 km) and could be crossed by the tidal incursion in the near (before 2038) or medium-term (after 2064) future under scenarios M3 and M2, respectively. If immediate action to halt channel deepening is taken (scenario M1) the TE will remain relatively constrained (TE < 70 km), for the majority of seasonal fresh-water flux conditions, until the end of the century.

4. Discussion and conclusions

Should channel bed lowering continue unmitigated, the TE in the Mekong delta will rapidly increase by ∼56 km in the next two decades. This dramatic landward expansion of the TE risks causing severe socioeconomic impacts, via exacerbation of saline intrusion (Smajgl *et al* 2015, Eslami *et al* 2019). Moreover, tidal extension will also affect delta channel stability and flood risk because of changes in bifurcation function (Zhang *et al* 2017) and water and sediment

routing (Nienhuis *et al* 2018). It is imperative, therefore, to identify correctly the dominant drivers of tidal extension in order to develop viable mitigation and adaptation strategies. Importantly, to date the dominant narrative has focused on the role of climate change in driving sea-level rise (Smajgl *et al* 2015, Ensign and Noe 2018) and land subsidence (Erban *et al* 2014, Minderhoud *et al* 2020) in driving tidal extension. Our results highlight that, although such factors do indeed contribute to tidal extension in the long term (i.e. by 2098), channel bed level lowering linked to cumulative anthropogenic sediment starvation, stemming from sand mining and damming, has a rapid and substantial influence that dominates all the other drivers of tidal extension combined. Critically, our findings demonstrate that present-day levels of channel bed level lowering stimulate such a powerful long-term commitment to tidal extension that, even if it is halted now, channel bed level lowering will continue to remain the net dominant driver of tidal extension until at least the end of the century. This means that attempts to mitigate against tidal extension must focus on reversing the negative sediment budgets that are driving channel bed level lowering. Our findings likely have widespread implications, as the Mekong is not the only large delta system that is sediment starved and which is highly vulnerable to tidal extension. Fluvial sediment reduction has been reported for many large rivers (Dunn *et al* 2019) and their deltas including the Chao Phraya (Winterwerp *et al* 2005, Saito *et al* 2007), Pearl (Zhang *et al* 2008a), Yangtze (Yang *et al* 2015) and Yellow (Wang *et al* 2010). It is clear that attempts to maintain climate resilient deltas globally will fail unless they include efforts to establish, sustain and enhance positive sediment budgets into their fragile systems.

Data availability statement

The data that support the findings of this study are openly available at the following URL: https://hydra.hull.ac.uk/resources/hull:17951.

Acknowledgments

ORCID iDs

G Vasilopoulos ⓘ https://orcid.org/0000-0003-1519-3442
I D Haigh ⓘ https://orcid.org/0000-0002-9722-3061

References

Anthony E J, Brunier G, Besset M, Goichot M, Dussouillez P and Nguyen ufV L 2015 Linking rapid erosion of the Mekong River delta to human activities *Sci. Rep.* **5** 1–12

Auerbach L W, Goodbred S L Jr, Mondal D R, Wilson C A, Ahmed K R, Roy K, Steckler M S, Small C, Gilligan J M and Ackerly B A 2015 Flood risk of natural and embanked landscapes on the Ganges–Brahmaputra tidal delta plain *Nat. Clim. Change* **5** 153–7

Bravard J P, Goichot M and Gaillot S 2013 Geography of sand and gravel mining in the Lower Mekong River. First survey and impact assessment *EchoGéo* Pôle de recherche pour l'organisation et la diffusion de l'information p 26

Bravard J P, Goichot M and Tronchère H 2014 An assessment of sediment-transport processes in the Lower Mekong River based on deposit grain sizes, the CM technique and flow-energy data *Geomorphology* **207** 174–89

Brunier G, Anthony E J, Goichot M, Provansal M and Dussouillez P 2014 Recent morphological changes in the Mekong and Bassac river channels, Mekong delta: the marked impact of river-bed mining and implications for delta destabilisation *Geomorphology* **224** 177–91

Chapman A, Darby S, Tompkins E, Hackney C, Leyland J, Tri Van P D, Pham T V, Parsons D, Aalto R and Nicholas A 2017 Sustainable rice cultivation in the deep flooded zones of the Vietnamese Mekong Delta *Vietnamese Sci. Technol.* **59** 34–8

Cheng Y and Andersen O B 2010 Improvement in global ocean tide model in shallow water regions *Poster, SV* pp 1–68

Church J A *et al* 2013 Sea level change *Climate Change 2013: The Physical Science Basis. Contribution of Working Group I to the Fifth Assessment Report of the Intergovernmental Panel on Climate Change* ed T F Stocker, D Qin, G K Plattner, M Tignor, S K Allen, J Boschung, A Nauels, Y Xia, V Bex and P M Midgley (Cambridge: Cambridge University Press) 1137–216

Dai Z and Liu J T 2013 Impacts of large dams on downstream fluvial sedimentation: an example of the Three Gorges Dam (TGD) on the Changjiang (Yangtze River) *J. Hydrol.* **480** 10–8

Darby S E, Hackney C R, Leyland J, Kummu M, Lauri H, Parsons D R, Best J L, Nicholas A P and Aalto R 2016 Fluvial sediment supply to a mega-delta reduced by shifting tropical-cyclone activity *Nature* **539** 276–9

Dunn F E, Darby S E, Nicholls R J, Cohen S, Zarfl C and Fekete B M 2019 Projections of declining fluvial sediment delivery to major deltas worldwide in response to climate change and anthropogenic stress *Environ. Res. Lett.* **14** 84034

Edmonds D A, Caldwell R L, Brondizio E S and Siani S M O 2020 Coastal flooding will disproportionately impact people on river deltas *Nat. Commun.* **11** 1–8

Edmonds D A and Slingerland R L 2008 Stability of delta distributary networks and their bifurcations *Water Resour. Res.* **44** 1–13

Ensign S H and Noe G B 2018 Tidal extension and sea-level rise: recommendations for a research agenda *Front. Ecol. Environ.* **16** 37–43

Erban L E, Gorelick S M and Zebker H A 2014 Groundwater extraction, land subsidence, and sea-level rise in the Mekong Delta, Vietnam *Environ. Res. Lett.* **9** 084010

Ericson J P, Vorosmarty C, Dingman S, Ward L and Meybeck M 2006 Effective sea-level rise and deltas: causes of change and human dimension implications *Glob. Planet. Change* **50** 63–82

Eslami S, Hoekstra P, Nguyen Trung N, Ahmed Kantoush S, van Binh D, Duc Dung D, Tran Quang T and van Der Vegt M 2019 Tidal amplification and salt intrusion in the Mekong Delta driven by anthropogenic sediment starvation *Sci. Rep.* **9** 1–10

Giosan L, Syvitski J, Constantinescu S and Day J 2014 Climate change: protect the world's deltas *Nat. News* **516** 31

Goodwin P, Haigh I D, Rohling E J and Slangen A 2017 A new approach to projecting 21st century sea-level changes and extremes *Earth's Future* **5** 240–53

Ha D T, Ouillon S and van Vinh G 2018 Water and suspended sediment budgets in the lower mekong from high-frequency measurements (2009–2016) *Water* **10** 846

Hackney C R, Darby S E, Parsons D R, Leyland J, Best J L, Aalto R, Nicholas A P and Houseago R C 2020 River bank instability from unsustainable sand mining in the lower Mekong River *Nat. Sustain.* **3** 217–25

Jordan C, Tiede J, Lojek O, Visscher J, Apel H, Nguyen H Q, Quang C N X and Schlurmann T 2019 Sand mining in the Mekong Delta revisited—current scales of local sediment deficits *Sci. Rep.* **9** 1–14

Kondolf G M, Rubin Z K and Minear J T 2014 Dams on the Mekong: cumulative sediment starvation *Water Resour. Res.* **50** 5158–69

Lan C W, Lo M H, Chou C and Kumar S 2016 Terrestrial water flux responses to global warming in tropical rainforest areas *Earth's Future* **4** 210–24

Legleiter C J and Kyriakidis P C 2008 Spatial prediction of river channel topography by kriging *Earth Surf. Process. Landf.* **33** 841–67

Merwade V M, Maidment D R and Goff J A 2006 Anisotropic considerations while interpolating river channel bathymetry *J. Hydrol.* **331** 731–41

Milliman J D and Meade R H 1983 World-wide delivery of river sediment to the oceans *J. Geol.* **91** 1–21

Minderhoud P S J, Middelkoop H, Erkens G and Stouthamer E 2020 Groundwater extraction may drown mega-delta: projections of extraction-induced subsidence and elevation of the Mekong delta for the 21st century *Environ. Res. Commun.* **2** 011005

Nash J E and Sutcliffe J V 1970 River flow forecasting through conceptual models part I—a discussion of principles *J. Hydrol.* **10** 282–90

Nienhuis J H, Hoitink A J F T and Törnqvist T E 2018 Future change to tide-influenced deltas *Geophys. Res. Lett.* **45** 3499–507

Oppenheimer M *et al* 2019 Sea level rise and implications for low lying Islands, coasts and communities (The Intergovernmental Panel on Climate Change)

Parry M *et al* 2007 *Climate Change 2007-Impacts, Adaptation and Vulnerability: Working Group II Contribution to the Fourth Assessment Report of the IPCC* (Cambridge University Press) pp 858–61

Saito Y, Chaimanee N, Thanawat J and Syvitski J P M 2007 Shrinking megadeltas in Asia: sea-level rise and sediment reduction impacts from case study of the chao phraya delta *Inprint Newsletter of the IGBP/IHDP Land Ocean Interaction in the Coastal Zone* vol 2 pp 3–9

Smajgl A, Toan T Q, Nhan D K, Ward J, Trung N H, Tri L Q, Tri V P D and Vu P T 2015 Responding to rising sea levels in the Mekong Delta *Nat. Clim. Change* **5** 167–74

Syvitski J P M 2008 Deltas at risk *Sustain. Sci.* **3** 23–32

Syvitski J P M *et al* 2009 Sinking deltas due to human activities *Nat. Geosci.* **2** 681–6

Szabo S *et al* 2016 Population dynamics, delta vulnerability and environmental change: comparison of the Mekong, Ganges–Brahmaputra and Amazon delta regions *Sustain. Sci.* **11** 539–54

Tamura T, Nguyen V L, Ta T K O, Bateman M D, Gugliotta M, Anthony E J, Nakashima R and Saito Y 2020 Long-term sediment decline causes ongoing shrinkage of the Mekong megadelta, Vietnam *Sci. Rep.* **10** 1–7

Tessler Z D, Vörösmarty C J, Overeem I and Syvitski J P M 2018 A model of water and sediment balance as determinants of relative sea level rise in contemporary and future deltas *Geomorphology* **305** 209–20

Törnqvist T E, Wallace D J, Storms J E A, Wallinga J, van Dam R L, Blaauw M, Derksen M S, Klerks C J W, Meijneken C and Snijders E M A 2008 Mississippi Delta subsidence primarily caused by compaction of Holocene strata *Nat. Geosci.* **1** 173–6

Vörösmarty C J and Sahagian D 2000 Anthropogenic disturbance of the terrestrial water cycle *BioScience* **50** 753

Vörösmarty C J, Syvitski J, Day J, De Sherbinin A, Giosan L and Paola C 2009 Battling to save the world's river deltas *Bull. At. Sci.* **65** 31–43

Wang H, Bi N, Saito Y, Wang Y, Sun X, Zhang J and Yang Z 2010 Recent changes in sediment delivery by the Huanghe (Yellow River) to the sea: causes and environmental implications in its estuary *J. Hydrol.* **391** 302–13

Winterwerp J C, Borst W G and de Vries M B 2005 Pilot study on the erosion and rehabilitation of a mangrove mud coast *J. Coast. Res.* **21** 223–30

Yang S L *et al* 2015 Decline of Yangtze River water and sediment discharge: impact from natural and anthropogenic changes *Sci. Rep.* **5** 1–14

Zhang S, Lu X X, Higgitt D L, Chen C T A, Han J and Sun H 2008a Recent changes of water discharge and sediment load in the Zhujiang (Pearl River) Basin, China *Glob. Planet. Change* **60** 365–80

Zhang W, Feng H, Hoitink A J F, Zhu Y, Gong F and Zheng J 2017 Tidal impacts on the subtidal flow division at the main bifurcation in the Yangtze River Delta *Estuar. Coast. Shelf Sci.* **196** 301–14

Zhang Y, Xue Y Q, Wu J C, Yu J, Wei Z X and Li Q F 2008b Land subsidence and earth fissures due to groundwater withdrawal in the Southern Yangtse Delta, China *Environm. Geol.* **55** 751